Asian Journal of Chemistry; Vol. 29, No. 3 (2017), 512-518

ASIAN JOURNAL OF CHEMISTRY

https://doi.org/10.14233/ajchem.2017.20238

Computational Studies on Thermodynamic Characteristics of $CH_3S(O)_nNO_2$ (n = 0-2) Compounds

J. CAO[*], Q. LI, Z.X. WANG, L.J. GAO, F. FU, B. FAN and Y. WANG

College of Chemistry & Chemical engineering, Shaanxi Key Laboratory of Chemical Reaction Engineering, Yan'an University, Yan'an 716000, Shaanxi Province, P.R. China

*Corresponding author: Tel/Fax: +86 911 2332037; E-mail: caojia213@126.com

Received: 16 August 2016; *Accepted*: 7 November 2016; *Published online*: 30 December 2016; AJC-18190

Geometries, frequencies and thermodynamic properties of some selected reference compounds are investigated using MP2, B3LYP, B3PW91 and PBEPBE methods with 6-311+G(3df,2p) basis set, respectively. The results indicate that the calculated structures and frequencies of various different methods are in good agreement with the available experimental data. The best agreement with experimental formation enthalpies is computed with the CBS-QB3 and CBS-Q methods. Several different methods are used to calculate the formation enthalpies, entropies and heat capacities of $CH_3S(O)_nNO_2$ (n = 0-2) species at 0 and 298 K, in which only $CH_3S(O)_2NO_2$ has the available theoretical formation enthalpy. The predicted entropies and heat capacities of $CH_3S(O)_nNO_2$ (n = 0-2) are based on the statistical mechanical principles from 200-2000 K. These data are essential to evaluate key atmospheric chemical processes of $CH_3S(O)_nNO_2$ (n = 0-2) compounds.

Keywords: $CH_3S(O)nNO_2$ (n = 0-2), Thermodynamic properties, Theoretical prediction.

INTRODUCTION

Dimethyl sulfide [CH_3SCH_3 (DMS)] is the most important sulfur compound in the atmosphere emitted from the oceans [1]. Atmospheric oxidation products of CH_3SCH_3 play a key role in aerosol formation and climate regulation [2]. Studies on the oxidation of CH_3SCH_3 are valuable to understand the sulfur cycle and therefore have been reported [3].

In the atmosphere, the main degradation process of CH_3SCH_3 is its reaction with OH radical during the daytime according to the following reaction channel [4-8],

$$CH_3SCH_3+OH \longrightarrow CH_3SCH_2+H_2O \quad (1)$$

$$CH_3SCH_2+O_2 \longrightarrow \text{Products} \quad (2)$$

$$CH_3SCH_3 + OH \longrightarrow CH_3S(OH)CH_3 \quad (3)$$

$$CH_3S(OH)CH_3 + O_2 \longrightarrow \text{Products} \quad (4)$$

The main products of eqns. 2 and 4 are CH_3SOCH_3, $CH_3SO_2CH_3$, CH_3SO_2H, SO_2, COS, CH_3SCHO and CH_3SO_3H. However, the distribution of these products is dependent on the ratio of the eqns. 2 and 4, which is affected by the NO_x(NO + NO_2) concentrations [9,10]. Patroescu *et al.* [9] found that the formation of CH_3SO_3H and $CH_3SO_2CH_3$ increase with the increasing NO_x(NO+NO_2) concentrations, whereas the yields of CH_3SOCH_3 and SO_2 decrease. Moreover, the higher NO_x levels play a significant role in the chemistry of intermediate CH_3SO_x [11], which is among the most intermediate in the atmosphere oxidation of CH_3SCH_3. Further reaction of CH_3SO_x with O_2 and NO_x is an important step resulting eventually in the formation of SO_2 and H_2SO_4 [12]. The favourable reactions of CH_3SO_x with O_2 and NO_x proceed *via* addition of O_2 and then NO_2 to CH_3SO_x, forming NO_2-containing organic sulfur compound [13]. $CH_3S(O)_2O_2NO_2$ is observed in the OH-radical initiated oxidation of CH_3SCH_3 even at low NO_x levels by the reaction of $CH_3S(O)_2O_2$ with NO_2 [9]. The experimental results indicated that CH_3SNO_2, CH_3SOONO_2 and $CH_3SO(O)ONO_2$ were measured [14-16]. These NO_2-containing organic sulfur compounds are important intermediates that link to the formation of acid rain in the atmosphere oxidation of CH_3SCH_3. Knowledge on thermodynamic properties is a key parameter in understanding the formation and destruction of atmospheric chemical processes of NO_2-containing organic sulfur compounds [17]. However, the experimental determination of thermodynamic properties is very difficult for the unstable species $CH_3S(O)_nNO_2$ (n = 0-2). Quantum chemistry method can help to obtain such properties [18]. To our best of knowledge, geometric structures, thermodynamic properties of $CH_3S(O)_nNO_2$ (n = 0-2) are few. Only formation enthalpy of single $CH_3S(O)_2NO_2$ were theoretical studied previously [12]. In present, the accuracy of various quantum chemical models to predict structures, vibrational frequencies, formation enthalpies, entropy and heat capacities is assessed. Then, we utilized several methods to calculate the thermodynamic and structural properties of $CH_3S(O)_nNO_2$ (n = 0-2) compound.

COMPUTATIONAL METHODS

All calculations have been Gaussian 09 program [19]. The geometries are optimized at the MP2 [20,21], B3LYP [22,23], B3PW91 and PBEPBE [24] levels of theory with the 6-311+G(3df,2p) basis set, respectively. Frequencies for all the studied molecules are calculated at the same level of theory. Enthalpies formation (Δ_fH^o) of the reactants and products are calculated by the atomization energy method at the MP2, B3LYP, B3PW91, PBEPBE, CBS-QB3 [25], G3 and G3MP2 [26] levels of theory, respectively. For any molecule, such as molecule M, the enthalpies of formation [$\Delta_fH^o_{(M,\,298\,K)}$] are given by eqn. 5 [27]:

$$\Delta_f H^o_{(M,298K)} = \sum_{atoms} \Delta_f H^o_{298K} + H^o_{298K}(M) - \sum_{atoms} H^o_{298K} \qquad (5)$$

where $\sum_{atoms} \Delta_f H^o_{298K}$ denotes experimental enthalpies of formation for the corresponding atoms are from reference [26], $\sum_{atoms} H^o_{298K}$ stands for the calculated enthalpies for the individual atoms, H^o_{298K} (M) is the calculated enthalpy of the molecule M. Entropies ($S^o_{298\,K}$) and heat capacities (C_p) are calculated using Multiwell program [28].

The theory of atom in molecule (AIM) is applied to investigate the bond properties [29]. The character of a bond may be described on the basis of the electron density (ρ) and its Laplacian ($\nabla^2\rho$) at the bond critical point [30]. Topological properties of a bond are characterized by the existence of a bond critical point (bcp) and the values of the electron density (ρ) and its Laplacian ($\nabla^2\rho$) at the bond critical point [31]. The negative value of $\nabla^2\rho$ indicates that the density is locally concentrated and characterizes a covalent bond. The positive value of $\nabla^2\rho$ indicates that the density is locally depleted and characterizes closed-shell interactions as found in ionic bonds, hydrogen bonds and van der Waals interactions [32]. The Multiwfn program has been used for the topological analysis of the electronic density [33,34].

RESULTS AND DISCUSSION

Initially, to test the accuracy of the methodology used in the present paper, we perform the calculation of some molecules for which their geometric parameters and frequency data are known [35]. The deviation from experiment by computed equilibrium bond lengths and bond angles for CH_3S, CH_3SH, CH_4, $^3O_2$, NO_2, CH_3NO_2, CH_3ONO_2 is investigated, respectively. Mean absolute deviations between the calculated respectively at the MP2/6-311+G(3df,2p), B3LYP/6-311+G(3df,2p), B3PW91/6-311+G(3df,2p), PBEPBE/6-311+G(3df,2p) levels of theory and the experimental are 0.005, 0.006, 0.007, 0.010 Å for bond lengths and 1.05, 1.20, 1.27, 1.28° for bong angles, respectively. The results suggested that the deviations of all the methods with the same basis set are minor and the MP2/6-311+G(3df,2p) method is the most accurate for the calculation of geometric parameters. The lowest energy structure is confirmed by harmonic vibrational frequency analysis, that is, all the frequencies of the stable structures are positive. Besides, the percentage errors including mean absolute percentage deviation and mean percentage deviation in calculated vibrational frequencies of the known reported species in present work are studied [35]. Mean absolute percentage deviations of MP2/6-311+G(3df,2p), B3LYP/6-311+G(3df,2p), B3PW91/6-311+G(3df,2p), PBEPBE/6-311+G(3df,2p) methods from the experiment are 3.48, 2.10, 2.41, 2.27, respectively. It can be found that B3LYP/6-311+G(3df,2p) and PBEPBE/6-311+G(3df,2p) frequencies are good agreement with the available experiment values, followed by B3PW91/6-311+G(3df,2p) method and the MP2/6-311+G(3df,2p) method. These results indicate the calculated structures and frequencies of above methods are accurate. For the purposes of our discussion, the MP2/6-311+G(3df,2p) results are used in the following geometric analysis. All optimized geometries at the MP2/6-31+G(2d,p) level are depicted in Fig. 1.

Molecular structures: Three isomers are found in CH_3SNO_2, which are labeled CH_3SNO_2, CH_3SONO-a and CH_3SONO-b, respectively. To search the possible conformer, the potential energy curves for CH_3SNO_2 and CH_3SONO-b are calculated by structure optimization at the specified dihedral angle (Fig. 2). In case of CH_3SNO_2, only one minimum with the C_s symmetry is obtained by scanning the dihedral O(2)NSC angle from 0° to 180° in steps of 10°. Similarly, the potential energy curve of CH_3SONO-b is calculated by structure optimization at fixed the dihedral SO(1)NO(2) angle from -180° to 180°. Fig. 2 showed that the potential energy curve of CH_3SONO-b with two minima at 0° (CH_3SONO-b)and 180° (CH_3SONO-a). CH_3SONO-a and CH_3SONO-b are *cis-trans* isomers. The energies of CH_3SONO-a and CH_3SONO-b are 4.16 and 3.16 kcal mol^{-1} higher than that of CH_3SNO_2 (using CBS-QB3 method), respectively. As for CH_3SONO_2, isomer $CH_3S(O)NO_2$, CH_3SONO_2-a and CH_3SONO_2-b are obtained, in which the order of their energy is $CH_3S(O)NO_2 > CH_3SONO_2$-a ≈ CH_3SONO_2-b. It is interesting that CH_3SONO_2-a and CH_3SONO_2-b are chiral isomers, which can be also confirmed by the potential energy curve of CH_3SONO_2 in Fig. 2. In $CH_3S(O)_2NO_2$, isomer $CH_3SO_2NO_2$ is more stable than isomers $CH_3S(O)ONO_2$ and CH_3SOONO_2.

Analysis of atoms in molecules (AIM) theory: The atom in molecule theory is an important tool to study the bond properties, which are characterized by the values of electron density (ρ) and its Laplacian ($\nabla^2\rho$) at the bond critical point. Table-2 lists the calculated values of ρ and $\nabla^2\rho$ in $CH_3S(O)_nNO_2$ (n = 0-2). To have a clear view of the bond critical point, the molecular graphs and contour lines of $\nabla^2\rho$ are also shown in Fig. 3. As seen in Table-1 and Fig. 3, the negative $\nabla^2\rho$ values of all the bonds in CH_3SNO_2 suggest the corresponding bonds have covalent character. In $CH_3S(O)_nNO_2$ (n = 1,2), the values of $\nabla^2\rho$ for all the S-O bonds have a ionic character due to the decentralization of electron density in the bond region with the positive values of $\nabla^2\rho$. For example, the topological values of S-O(1) in $CH_3S(O)NO_2$ are r = 0.3006 and $\nabla^2\rho$ = 0.8055 a.u, pointing out the ionic character. Additionally, the strength of the bond can be estimated from the magnitude of ρ at the bond critical point. The ρ value of N-O(1) bond is larger than that of the N-O(2) bond in CH_3SONO_2-a compound, which indicates the N-O(1) bond is stronger than N-O(2) bond.

Enthalpy of formation: Enthalpy of formation is the important fundamental properties of a molecule, which is usually taken as the key parameters for modeling of the formation

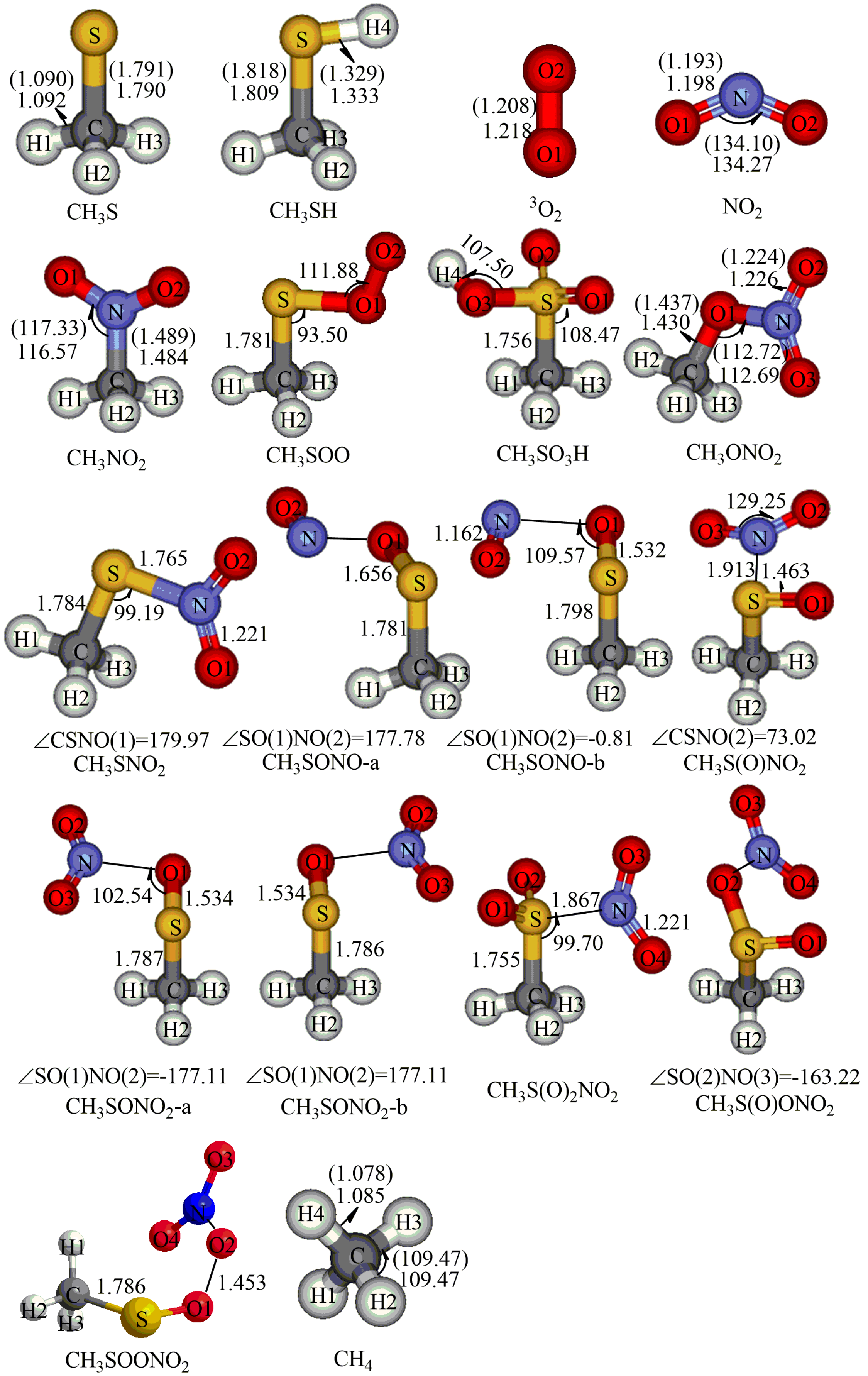

Fig. 1. Optimized geometries of all the species at the MP2/6-31+G(3df,2p) level of theory along with the available experimental values in the parentheses from the reference [34]. Bond lengths are in angstroms and angles are in degrees

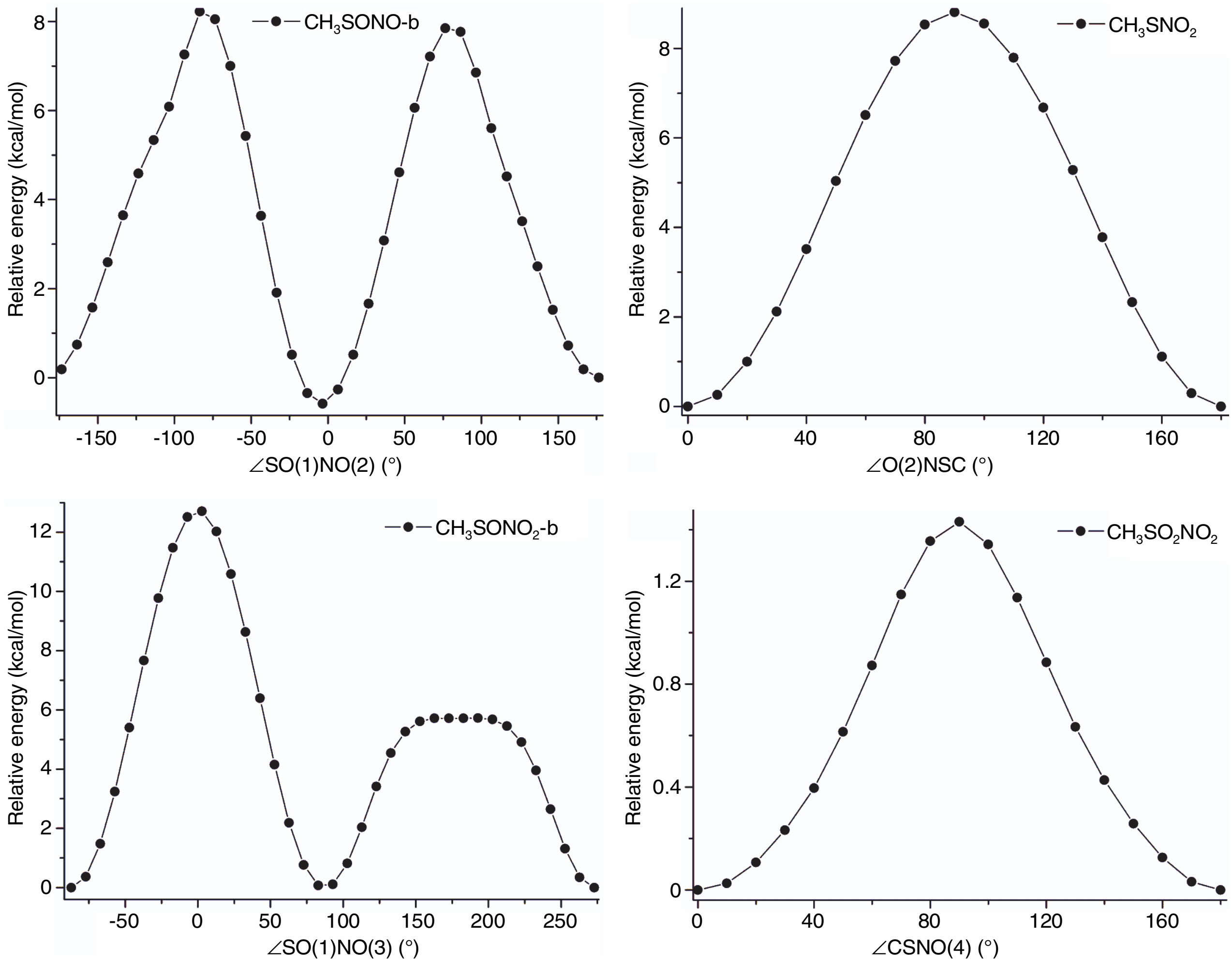

Fig. 2. Potential energy curves calculated at the MP2/6-311+G(3df,2p) level. Every molecular coordinate was fully relaxed except the scanned torsional angle

TABLE-1
BOND CRITICAL POINT PROPERTIES OF ELECTRON DENSITY (ρ), ITS LAPLACIAN ($\nabla^2\rho$) AND THE LOCAL ENERGY DENSITY OF THE TITLED COMPOUNDS CALCULATED AT THE MP2/6-311+G(3df,2p) LEVEL

Bond	CH_3SNO_2		CH_3SONO-a		CH_3SONO-b		$CH_3S(O)NO_2$		CH_3SOONO_2	
	ρ	$\nabla^2\rho$	ρ	$\nabla^2\rho$	ρ	$\nabla^2\rho$	ρ	$\nabla^2\rho$	ρ	$\nabla^2\rho$
C-H(1)	0.2866	-1.0729	0.2905	-1.0998	0.2879	-1.0807	0.2908	-1.1063	0.2923	-1.1127
C-H(2)	0.2941	-1.1284	0.2855	-1.0650	0.2864	-1.0721	0.2892	-1.0920	0.2851	-1.0619
C-H(3)	0.2941	-1.1284	0.2910	-1.1035	0.2898	-1.0944	0.2902	-1.1022	0.2926	-1.1169
C-S	0.2048	-0.4391	0.2065	-0.4575	0.2057	-0.4613	0.2133	-0.4920	0.2065	-0.4526
S-N	0.1873	-0.1720					0.1542	-0.2388		
S-O(1)			0.1949	0.1767	0.2540	0.5860	0.3006	0.8055	0.1945	0.2745
N-O(1)	0.5274	-1.3269	0.2352	-0.1472	0.0628	0.1571				
N-O(2)	0.5267	-1.3114	0.6256	-2.4712	0.5987	-2.2553	0.5361	-1.3999	0.2897	-0.3830
N-O(3)							0.5286	-1.3577	0.5600	-0.1436

Bond	CH_3SONO_2-a		CH_3SONO_2-b		$CH_3S(O)_2NO_2$		$CH_3S(O)ONO_2$	
	ρ	$\nabla^2\rho$	ρ	$\nabla^2\rho$	ρ	$\nabla^2\rho$	ρ	$\nabla^2\rho$
C-H(1)	0.2879	-1.0818	0.2899	-1.0964	0.2936	-1.1315	0.2888	-1.0899
C-H(2)	0.2868	-1.0758	0.2868	-1.0758	0.2936	-1.1315	0.2880	-1.0810
C-H(3)	0.2899	-1.0964	0.2879	-1.0817	0.2882	-1.0875	0.2941	-1.1322
C-S	0.2101	-0.4774	0.2101	-0.4773	0.2304	-0.5812	0.2164	-0.5114
S-N					0.1764	-0.4104		
S-O(1)	0.2472	0.6750	0.2472	0.6751	0.3270	0.9936	0.3037	0.7838
S-O(2)					0.3270	0.9936	0.1858	-0.0488
N-O(1)	0.0826	0.1660	0.0826	0.1660				
N-O(2)	0.5581	-1.5005	0.5582	-1.5008			0.2831	-0.3476
N-O(3)	0.5602	-1.5724	0.5602	-1.5722	0.5329	-1.3577	0.5652	-1.4732
N-O(4)					0.5259	-1.3326	0.5578	-1.4310

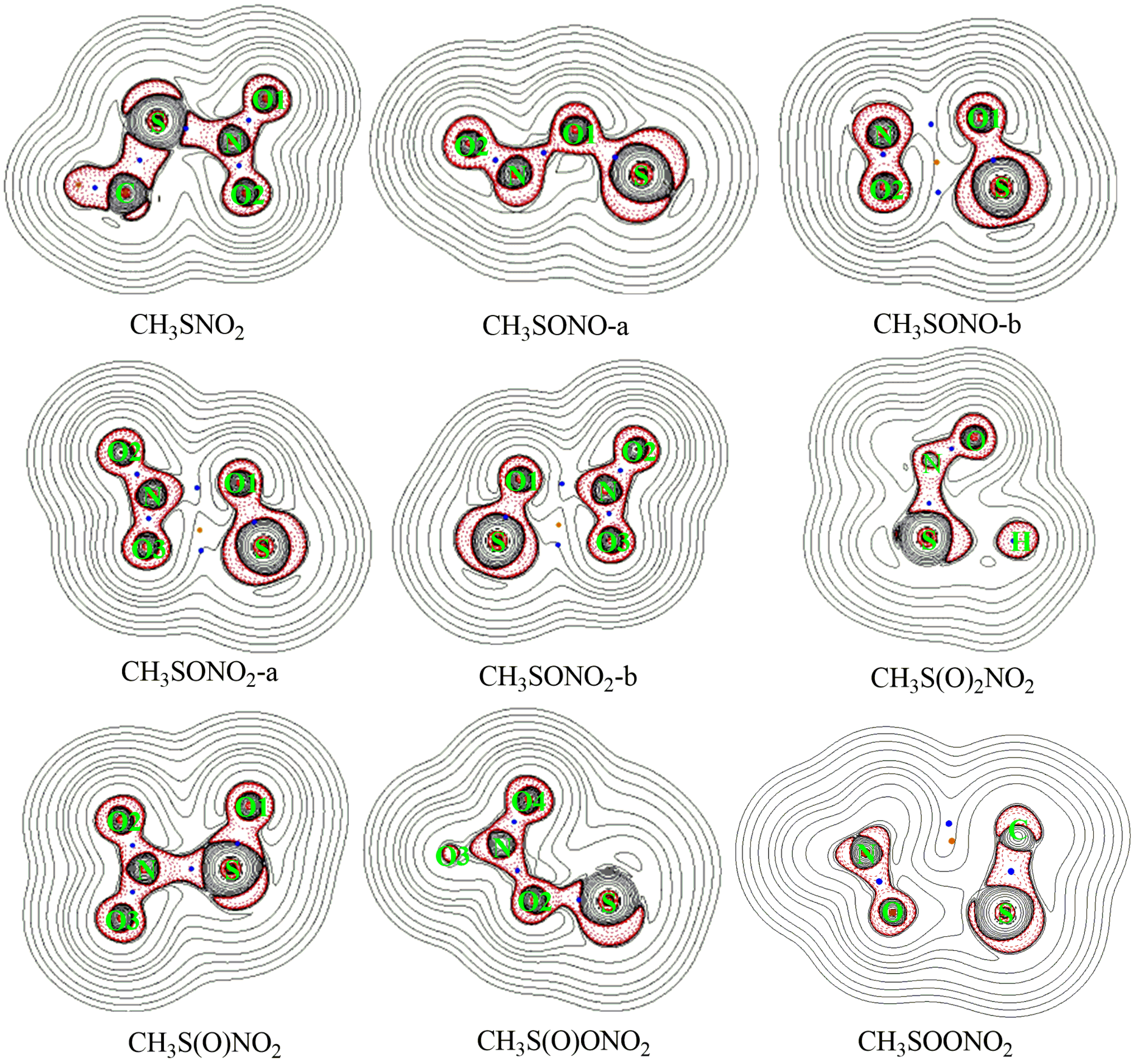

CH_3SNO_2 CH_3SONO-a CH_3SONO-b

CH_3SONO_2-a CH_3SONO_2-b $CH_3S(O)_2NO_2$

$CH_3S(O)NO_2$ $CH_3S(O)ONO_2$ CH_3SOONO_2

Fig. 3. Molecular structure of the $CH_3S(O)_nNO_2$ (n = 0-2), ring critical points and bond critical points are represented by small yellow and orange spheres, respectively

and destruction of the organic sulfur pollutant in atmosphere. The gas phase enthalpies of formation of $CH_3S(O)_nNO_2$ (n = 0-2) compounds at 0 and 298 K have been predicted by using atomization reaction method. Table-2 lists the deviation from experiment by calculated enthalpy of formation for ten test molecules (CH_3S, CH_3SH, CH_4, $^3O_2$, NO_2, CH_3NO_2, CH_3ONO_2, CH_3SOO, CH_3SO_3H) for which their $\Delta_fH^{\circ}_{298\ K}$ is known [35-37]. On the basis of mean absolute deviation (MAD), the best performance is obtained with the CBS-QB3 and CBS-Q methods, MAD = 1.39 and 1.51 kcal mol^{-1}, followed by MAD = 3.09, 3.39, 3.87, 3.97, 6.00 and 24.82 kcal mol^{-1}, respectively, for G3MP2B3, G3MP2, B3LYP, B3PW91, MP2, PBEPBE, respectively. The PBEPBE method significantly underestimates the formation enthalpies of CH_3NO_2 and CH_3ONO_2. The overall accuracies of CBS-QB3, CBS-Q, G3MP2B3, G3MP2 methods exceed that of B3LYP, B3PW91, MP2 and PBEPBE results. Our recommended $\Delta_fH^{\circ}_{298\ K}$ values of -3.37, 0.80, -0.20, -14.27, -14.27, -30.11 kcal mol^{-1} for CH_3SNO_2, CH_3SONO-a, CH_3SONO-b, CH_3SONO_2-a, CH_3SONO_2-b, $CH_3S(O)NO_2$ at the CBS-QB3 method (Table-3). Our calculated formation enthalpies of $CH_3S(O)_2NO_2$ at 298 K (-73.53 kcal mol^{-1})is consistent with previous only calculation (-73.7 kcal mol^{-1}) [12]. This overall agreement confirms the reliability of our computational results.

Entropy ($S^{\circ}_{298\ K}$) and heat capacity [$C_p(T)$]: Entropy ($S^{\circ}_{298\ K}$) and heat capacities (C_p) for $CH_3S(O)_nNO_2$ (n = 0-2) molecules are listed in Table-4. As there is no experimental or theoretical information of $S^{\circ}_{298\ K}$ and C_p for the $CH_3S(O)_nNO_2$ (n = 0-2) compounds. The accuracy of the predicted is checked by comparing the calculated $S^{\circ}_{298\ K}$ and C_p (298 K) of five test sets with available experimental values (Table-5). The calculated $S^{\circ}_{298\ K}$ and C_p for the species (CH_3SH, CH_4, $^3O_2$, NO_2, CH_3NO_2) are in line with the corresponding experiment values [34]. The maximum deviations of $S^{\circ}_{298\ K}$ and C_p (298 K) are 3.96 (in CH_3NO_2) and 0.23 cal mol^{-1} K^{-1} (in CH_3SH).

Conclusion

The geometric structures and thermodynamic properties (including formation enthalpies, entropies and heat capacities) of $CH_3S(O)_nNO_2$ (n = 0-2) compounds are calculated using

TABLE-2
THE CALCULATED ENTHALPIES OF FORMATION ($\Delta_f H^O_{298\ K}$) (kcal mol^{-1}) FROM THE ATOMIZATION ENERGY METHOD

Species	Exp. [36,37]	$\Delta_f H^O_{298\ K}$							
		MP2	B3LYP	B3PW91	PBEPBE	CBS-Q	CBS-QB3	G3MP2	G3MP2B3
		6-311+G(3df,2p)							
CH_3S	29.67	41.10	29.92	28.32	22.15	30.15	29.87	29.85	29.63
CH_3SH	-5.45	10.60	-1.55	-2.90	-8.86	-4.25	-4.56	-4.09	-4.08
CH_4	-17.81	-3.33	-17.13	-15.68	-17.07	-16.52	-16.64	-16.65	-16.42
$^3O_2$	0.00	-6.28	-2.51	-3.91	-22.59	0.88	0.35	3.22	1.62
NO_2	7.90	6.79	3.24	1.25	-34.11	7.39	7.75	10.92	10.10
CH_3NO_2	-17.79	-19.73	-18.06	-20.91	-58.85	-16.92	-17.63	-13.74	-14.65
CH_3ONO_2	-28.50	-35.45	-29.81	-34.18	-84.50	-29.18	-29.99	-24.37	-25.63
CH_3SO	-15.95	-6.27	-14.32	-17.10	-35.41	-17.37	-17.05	-15.53	-15.12
CH_3SOO	18.02	36.42	21.47	18.52	-15.14	21.68	22.72	24.14	25.14
CH_3SO_3H	-133.90	-131.30	-113.88	-121.24	-156.14	-129.83	-130.23	-123.71	-123.62
Mean deviation		5.64	2.12	-0.40	-24.67	0.98	0.84	3.39	3.08
Mean absolute deviation		6.00	3.87	3.97	24.82	1.51	1.39	3.39	3.09

TABLE-3
THE CALCULATED ENTHALPIES OF FORMATION ($\Delta_f H^O$) (kcal mol^{-1}) FROM THE ATOMIZATION ENERGY METHOD

Species	$\Delta_f H^O_{298\ K}$							
	MP2	B3LYP	B3PW91	PBEPBE	CBS-Q	CBS-QB3	G3MP2	G3MP2B3
	6-311+G(3df,2p)							
CH_3SNO_2	-4.57	-1.83	-7.34	-53.43	-3.33	-3.37	0.69	0.12
CH_3SONO-a	3.85	4.10	1.25	-44.65	0.45	0.80	4.24	3.43
CH_3SONO-b	-3.15	3.50	0.45	-46.74	-0.44	-0.20	5.60	2.87
CH_3SONO_2-a	-22.41	-11.19	-17.32	-78.91	-13.82	-14.27	-7.94	-9.17
CH_3SONO_2-b	-22.41	-11.19	-17.32	-78.91	-13.82	-14.27	-7.94	-9.17
$CH_3S(O)NO_2$	-38.38	-26.81	-33.15	-92.54	-30.38	-30.11	-25.19	-25.89
$CH_3S(O)_2NO_2$	-88.89	-63.23	-72.97	-140.69	-73.76	-73.53	-65.39	-66.04
$CH_3S(O)ONO_2$	-58.32	-40.40	-48.32	-118.78	-46.56	-46.96	-39.33	-40.43
CH_3SOONO_2	-3.21	-42.92	-51.14	-120.47	3.06	0	9.56	7.93
	$\Delta_f H^O_{0\ K}$							
CH_3SNO_2	-4.24	-1.60	-7.08	-53.28	-3.02	-3.20	0.95	0.25
CH_3SONO-a	3.61	3.89	1.09	-45.01	0.42	0.55	4.16	3.19
CH_3SONO-b	-3.25	3.25	0.30	-47.07	-0.37	-0.44	5.62	2.69
CH_3SONO_2-a	-22.68	-11.34	-17.37	-79.27	-13.65	-14.42	-7.83	-9.31
CH_3SONO_2-b	-22.68	-11.34	-17.37	-79.27	-13.65	-14.42	-7.83	-9.31
$CH_3S(O)NO_2$	-38.37	-26.93	-33.22	-92.80	-30.26	-30.28	-25.13	-26.13
$CH_3S(O)_2NO_2$	-88.80	-63.28	-72.97	-140.93	-73.62	-73.71	-65.31	-66.29
$CH_3S(O)ONO_2$	-58.47	-40.59	-48.45	-119.34	-46.51	-47.20	-39.35	-40.70
CH_3SOONO_2	-3.39	-43.02	-51.18	-120.74	7.75	5.98	14.25	12.62

TABLE-4
ENTROPY ($S^o_{298\ K}$, cal mol^{-1} K^{-1}) AND HEAT CAPACITY (C_p, cal mol^{-1} K^{-1})

Species	$S^O_{298\ K}$	C_P									
		200	298	400	600	800	1000	1200	1400	1700	2000
CH_3SNO_2	76.16	16.26	20.01	23.55	28.86	32.44	34.96	36.79	38.15	39.59	40.57
CH_3SONO-a	79.27	18.35	21.98	25.16	29.83	33.04	35.36	37.08	38.37	39.75	40.68
CH_3SONO-b	79.70	18.44	22.04	25.21	29.85	33.05	35.37	37.08	38.37	39.74	40.67
CH_3SONO_2-a	83.45	19.93	24.38	28.36	34.10	37.91	40.58	42.50	43.93	45.42	46.43
CH_3SONO_2-b	83.46	19.93	24.38	28.36	34.11	37.91	40.58	42.50	43.93	45.42	46.43
$CH_3S(O)NO_2$	82.86	19.97	24.29	28.19	33.97	37.83	40.52	42.46	43.89	45.40	46.41
$CH_3S(O)_2NO_2$	87.27	21.69	26.85	31.45	38.20	42.64	45.66	47.82	49.39	51.03	52.12
$CH_3S(O)ONO_2$	88.11	22.10	27.63	32.36	38.97	43.19	46.07	48.12	49.62	51.20	52.25
CH_3SOONO_2	86.85	21.76	27.23	32.03	38.78	43.08	46.00	48.07	49.59	51.18	52.24

various different theoretical methods (MP2, B3LYP, PBEPBE, B3PW91, CBS-Q, CB3-QB3, G3MP2, G3MP2B3). Nine isomers are found for $CH_3S(O)_nNO_2$ (n = 0-2). The structural results from methods of MP2, B3LYP, PBEPBE and B3PW91 are in line with available experimental data. The atom in molecule calculations are performed in order to analyze bond properties of the titled compound. The formation enthalpies results indicated that the accuracy of composite methods (CBS-Q, CBS-QB3, G3MP2, G3MP2B3) are higher than that of other methods (MP2, B3LYP, PBEPBE, B3PW91).

TABLE-5
ENTROPY($S^o_{298\ K}$, cal mol^{-1} K^{-1}) AND
HEAT CAPACITY (C_p, cal mol^{-1} K^{-1})

Species	$S^o_{298\ K}$	C_p (298 K)^a
CH_3SH	60.64 (60.74)	12.19 (11.96)
CH_4	44.46 (44.37)	8.45 (8.49)
$^3O_2$	46.79 (48.84)	7.00 (6.99)
NO_2	57.28 (57.18)	8.80 (8.85)
CH_3NO_2	69.48 (65.52)	14.51

^{a}The values in the parentheses from the references [35]

ACKNOWLEDGEMENTS

The authors thank National Natural Science Foundation of China (21543017), Foundation of Yan'an University (YDQ2014-32), College of Chemistry & Chemical Engineering of Yan'an University (YDHG2014-Z04), Innovation and Entrepreneurship Training Program of College Students of Shaanxi Province in 2015 (1449) and National College Students' Innovative Entrepreneurial Training Plan (201510719288) for financial support. The authors also thank Shanghai Supercomputer Center for accessing the high performance computing service and program support.

REFERENCES

1. H. Falbe-Hansen, S. Sørensen, N.R. Jensen, T. Pedersen and J. Hjorth, *Atmos. Environ.*, **34**, 1543 (2000).
2. V. Librando, G. Tringali, J. Hjorth and S. Coluccia, *Environ. Pollut.*, **127**, 403 (2004).
3. I. Barnes, J. Hjorth and N. Mihalopoulos, *Chem. Rev.*, **106**, 940 (2006).
4. S. Jørgensen and H.G. Kjaergaard, *J. Phys. Chem. A*, **114**, 4857 (2010).
5. J.M. Ramirez-Anguita, A.S. Gonzalez-Lafont and J.M. Lluch, *Comput. Theor. Chem.*, **965**, 249 (2011).
6. J.M. Ramirez-Anguita, A.S. Gonzalez-Lafont and J.M. Lluch, *J. Comput. Chem.*, **32**, 2104 (2011).
7. J.M. Ramirez-Anguita, A.S. Gonzalez-Lafont and J.M. Lluch, *J. Comput. Chem.*, **30**, 1477 (2009).
8. L. Zhu, J.M. Nicovich and P.H. Wine, *J. Phys. Chem. A*, **109**, 3903 (2005).
9. I.V. Patroescu, I. Barnes, K.H. Becker and N. Mihalopoulos, *Atmos. Environ.*, **33**, 25 (1998).
10. C. Arsene, I. Barnes, K.H. Becker and R. Mocanu, *Atmos. Environ.*, **35**, 3769 (2001).
11. D. Grosjean, *Environ. Sci. Technol.*, **18**, 460 (1984).
12. Z. Salta, A.M. Kosmas and A. Lesar, *Comput. Theor. Chem.*, **1001**, 67 (2012).
13. Z.H. Shon and K.H. Kim, *Chemosphere*, **63**, 1859 (2006).
14. G.S. Tyndall and A.R. Ravishankara, *J. Phys. Chem.*, **93**, 2426 (1989).
15. N.R. Jensen, J. Hjorth, C. Lohse, H. Skov and G. Restelli, *Atmos. Environ.*, **25**, 1897 (1991).
16. A. Turnipseed, S.B. Barone and A.R. Ravishankara, *J. Phys. Chem.*, **96**, 7502 (1992).
17. D.K. Hahn, K.S. Raghu Veer and J.V. Ortiz, *J. Phys. Chem. A*, **114**, 8142 (2010).
18. V. van Speybroeck, R. Gani and R.J. Meier, *Chem. Soc. Rev.*, **39**, 1764 (2010).
19. M.J. Frisch, G.W. Trucks, H.B. Schlegel, G.E. Scuseria, M.A. Robb, J.R. Cheeseman, G. Scalmani, V. Barone, B. Mennucci, G. A. Petersson, H. Nakatsuji, M. Caricato, X. Li, H.P. Hratchian, A.F. Izmaylov, J. Bloino, G. Zheng, J.L. Sonnenberg, M. Hada, M. Ehara, K. Toyota, R. Fukuda, J. Hasegawa, M. Ishida, T. Nakajima, Y. Honda, O. Kitao, H. Nakai, T. Vreven, J.A. Montgomery Jr., J.E. Peralta, F. Ogliaro, M. Bearpark, J.J. Heyd, E. Brothers, K.N. Kudin, V.N. Staroverov, R. Kobayashi, J. Normand, K. Raghavachari, A. Rendell, J.C. Burant, S.S. Iyengar, J. Tomasi, M. Cossi, N. Rega, J.M. Millam, M. Klene, J.E. Knox, J.B. Cross, V. Bakken, C. Adamo, J. Jaramillo, R. Gomperts, R.E. Stratmann, O. Yazyev, A.J. Austin, R. Cammi, C. Pomelli, J.W. Ochterski, R.L. Martin, K. Morokuma, V.G. Zakrzewski, G.A. Voth, P. Salvador, J.J. Dannenberg, S. Dapprich, A.D. Daniels, Ö. Farkas, J.B. Foresman, J.V. Ortiz, J. Cioslowski and D.J. Fox, GAUSSIAN 09, Revision C.02, Gaussian, Inc., Pittsburgh, PA (2009).
20. C. Møller and M.S. Plesset, *Phys. Rev.*, **46**, 618 (1934).
21. M. Head-Gordon, J.A. Pople and M.J. Frisch, *Chem. Phys. Lett.*, **153**, 503 (1988).
22. A.D. Becke, *J. Chem. Phys.*, **98**, 5648 (1993).
23. C. Lee, W. Yang and R.G. Parr, *Phys. Rev. B*, **37**, 785 (1988).
24. J.P. Perdew, K. Burke and M. Ernzerhof, *Phys. Rev. Lett.*, **77**, 3865 (1996).
25. J.A. Montgomery, M.J. Frisch, J.W. Ochterski and G.A. Petersson, *J. Chem. Phys.*, **110**, 2822 (1999).
26. L.A. Curtiss, P.C. Redfern, K. Raghavachari, V. Rassolov and J.A. Pople, *J. Chem. Phys.*, **110**, 4703 (1999).
27. L.A. Curtiss, K. Raghavachari, P.C. Redfern and J.A. Pople, *J. Chem. Phys.*, **106**, 1063 (1997).
28. J.R. Barker, N.F. Ortiz, J.M. Preses, L.L. Lohr, A. Maranzana, P.J. Stimac, T.L. Nguyen and T.J. Dhilip Kumar, MultiWell-2010 Software (2010).
29. R.F.W. Bader, Atoms in Molecules. A Quantum Theory, Oxford University Press, New York (1994).
30. J. Gonzalez, M.J. Torrent-Sucarrat and M. Anglada, *Phys. Chem. Chem. Phys.*, **12**, 2116 (2010).
31. H.S. Biswal, P.R. Shirhatti and S. Wategaonkar, *J. Phys. Chem. A*, **113**, 5633 (2009).
32. J. Andres, P. Gonzalez-Navarrete and V.S. Safont, *Int. J. Quantum Chem.*, **114**, 1239 (2014).
33. T. Lu and F.W. Chen, *J. Comput. Chem.*, **33**, 580 (2012).
34. T. Lu and F.W. Chen, *J. Mol. Graph. Model.*, **38**, 314 (2012).
35. R.D. Johnson III, NIST Standard Reference Database Number 101, Release 16a, July (2016).
36. R. Atkinson, D.L. Baulch, R.A. Cox, J.N. Crowley, R.F. Hampson, R. Hynes, M.E. Jenkin, M.J. Rossi and J. Troe, *Atmos. Chem. Phys.*, **4**, 1461 (2004).
37. M. Frenkel, G.J. Kabo, K.N. Marsh, G.N. Roganov and R.C. Wilhoit, Thermodynamics of Organic Compounds in the Gas State, Thermodynamics Research Center, College Station, TX (1994).